

# Resonant excitation of intraband absorption in InAs/GaAs self-assembled quantum dots

S. Sauvage and P. Boucaud<sup>a)</sup>

*Institut d'Electronique Fondamentale, URA CNRS 22, Bât. 220, Université Paris-Sud, 91405 Orsay, France*

J.-M. Gérard

*France Telecom, CNET Bagneux, 196 Av H. Ravera, 92225 Bagneux, France*

V. Thierry-Mieg

*Laboratoire de Microstructures et Microélectronique, UPR CNRS 20, 196 Av H. Ravera, 92225 Bagneux, France*

(Received 12 May 1998; accepted for publication 11 July 1998)

We have investigated the infrared absorption between confined levels in the conduction and valence bands of undoped InAs/GaAs self-assembled quantum dots. The intraband absorption, which is measured by photoinduced spectroscopy, is analyzed under resonant and nonresonant optical excitation of the quantum dots. The assignment of electron and hole intraband transitions is achieved on the basis of experimental results obtained with *n*- and *p*-doped quantum dots. A careful analysis of the absorption spectra shows that several hole transitions and one electron transition with a large broadening are evidenced in the mid-infrared spectral range. We show that the amplitude of the intraband absorption depends on the pump excitation wavelength and exhibits a maximum when the dots are populated via the wetting layer. The spectral shape of the hole intraband absorption is very weakly dependent on the excitation wavelength. The amplitude of the photoinduced hole intraband absorption exhibits a sublinear behavior with the pump intensity. This feature is explained by the state filling of the quantum dots. © 1998 American Institute of Physics.

[S0021-8979(98)02520-1]

## I. INTRODUCTION

Self-assembled quantum dots are semiconductor heterostructures where the carriers are spatially confined in the three space directions. The formation of the self-assembled clusters is based on a strain-driven mechanism between highly mismatched semiconductors. The coherent clusters appear beyond a critical thickness of the deposited layer when the growth mode switches from a 2D layer-by-layer growth mode to a 3D growth mode. The three-dimensional confining potential leads to several distinctive features as compared to bulk semiconductors or quantum well heterostructures. The 3D nanostructures have an atomic-like discrete density of states and the energy spectrum consists of a series of quantized atomlike levels in the conduction and in the valence bands.<sup>1,2</sup>

The most widely used optical characterization of the self-assembled quantum dots is photoluminescence (PL). Photoluminescence gives valuable information on the size distribution and the energy spectrum of the clusters. The radiative recombination of carriers between the ground and excited states in the valence and conduction band can be easily evidenced by continuous-wave photoluminescence.<sup>3,4</sup> Time-resolved photoluminescence allows the determination of the capture and recombination time of the carriers in the quantum dots.<sup>5,6</sup> The photoluminescence of a single quantum dot has been observed by spatially-resolved photolumines-

cence and gives, in turn, direct information on the  $\delta$ -like density of states of the clusters.<sup>1,2</sup> However, the photoluminescence corresponds to a radiative recombination where both electrons or holes are involved. Therefore, it is difficult to disentangle only by photoluminescence the intrinsic properties and energy structure of the carriers confined in the conduction band and in the valence band. Additional information on the energy spectrum and the relaxation mechanisms of the carriers within the quantum dots can be obtained by photoluminescence excitation spectroscopy or by resonant photoluminescence spectroscopy. In the latter case, the low-temperature photoluminescence of the inhomogeneously broadened cluster distribution generally leads to several distinctive features. Fluorescence-line narrowing has been reported in CdSe quantum dots.<sup>7</sup> In the case of InGaAs islands grown on GaAs substrates, the resonant photoluminescence exhibits some well-defined maxima which are energetically separated by fixed values.<sup>8,9</sup> The replica appear at energies which match a multiple of phonon energies and have been attributed to the multiphonon relaxation mechanisms which occur in the clusters. Note that the presence of the replica at multiple phonon energies in resonant photoluminescence depends on the size and shape of the semiconductor clusters since it is not systematically observed.<sup>5</sup> Nonetheless, resonant photoluminescence is a powerful technique to study in more detail the electron and hole relaxation mechanisms and the energy diagram of the quantum dots.

To further analyze the energy spectrum of the quantum dots, the study of intraband transitions has been considered

<sup>a)</sup>Electronic mail: phill@ief.u-psud.fr

by several authors. The intraband transitions involve dipole-allowed transitions between discrete confined states lying in the same band, either the conduction band or the valence band. Therefore, they can provide unambiguous and separate information on the energy structure of the electrons and the holes confined in the quantum dots. Intraband transitions have been first observed by magnetospectroscopy in a patterned array of InSb quantum dots.<sup>10</sup> In the case of InAs/GaAs quantum dots, intraband transitions within the conduction band have been observed by far-infrared spectroscopy coupled to a capacitance charging method.<sup>11</sup> The energy shell structure of the quantum dots has been deduced from these experiments. It was shown in these quantum dots that the energy diagram was similar to the one corresponding to a parabolic potential confinement. Recently, we have demonstrated that both electron and hole intraband transitions can be observed in the mid-infrared spectral range by photoinduced spectroscopy.<sup>12</sup> In the latter case, the InAs quantum dots were populated using an interband optical excitation with an energy above the band gap of the wetting layer.

The purpose of this article is to investigate in detail the dependence of the photoinduced intraband absorption in quantum dots as a function of the interband optical pump energy. The energy of the interband optical pump is varied over a wide range which covers the GaAs band gap, the wetting layer energy, the excited states of the quantum dots and the ground state energies of the dots. We show that the intraband absorption is enhanced when the dots are directly populated via the wetting layer. The energy position and spectral broadening of the intraband transitions weakly depend on the excitation wavelength. The amplitude of the intraband absorption exhibits a sublinear dependence with the interband pump intensity. The dependence on the pump intensity is explained by the state filling of the quantum dots. The results reported on the resonant excitation of the intraband absorption are correlated with resonant photoluminescence measurements.

This article is presented as follows: Sec. II is devoted to the sample growth and the experimental technique. Section III deals with the assignment of the intraband transitions observed by photoinduced spectroscopy by comparison with direct intraband absorption measurements in doped samples. The dependence of the intraband absorption amplitude on the pump wavelength is reported in Sec. IV. Sections V and VI tackle the resonant excitation of the dots as observed by photoluminescence or intraband absorption spectroscopy. Finally, the dependence of the intraband absorption on the pump intensity is discussed in Sec. VII.

## II. SAMPLES AND EXPERIMENTAL TECHNIQUE

The samples were grown by molecular beam epitaxy on (001)-oriented GaAs substrates.<sup>12</sup> They consist of 30 InAs layers separated by GaAs barriers. One sample (sample B) has only 10 InAs layers. The growth temperature was 520 °C under As<sub>2</sub> or As<sub>4</sub> arsenic beam. Under the present growth conditions, the dot carrier density is estimated to be  $4 \times 10^{10} \text{ cm}^{-2}$ . One of the sample (sample A<sub>2</sub>) has been extracted from a wafer which was not rotated during growth.<sup>12</sup>

along this wafer, the local average size of the dots varies continuously and enables the study of different size distributions. Note that, on the other hand, the dot density can be reduced when we approach the frontier between the 3D-2D growth mode transition.<sup>13,14</sup> The photoluminescence of the undoped samples has been reported in a previous article.<sup>12</sup> The doping of the samples was achieved with either a silicon or a beryllium  $\delta$  doping lying 2 nm below the InAs wetting layer. The bidimensional carrier density in the  $\delta$ -doped layer was  $\sim 8 \times 10^{10} \text{ cm}^{-2}$  which corresponds, after spatial transfer, to the complete filling of the dot ground state.

Transmission electron microscopy shows that the dots have a plano-convex geometry.<sup>6</sup> The base length varies between 15 and 25 nm with an height between 2 and 3 nm. The aspect ratio (height divided by base length) is rather low for the present clusters. Depending on the growth conditions, different shapes and geometries which include square-based pyramids,<sup>2</sup> and lenses<sup>6,15</sup> have been reported in the literature. In all cases, the sizes are sufficiently small to lead to strong quantum confinement effects. However, the issues of the shape and facet orientation are of crucial importance for the study of the intraband transitions in the quantum dots. The energy ladder and the polarization selection rules strongly depend on the confinement potential (i.e., parabolic potential or not). This problem has been partially investigated in Ref. 16. In this article, the energy diagram was calculated for pyramids with different aspect ratios. As expected, the origin of the different interband optical transitions was strongly dependent on the shape of the dots.

The infrared absorption measurements are performed with a mid-infrared Fourier transform spectrometer. In order to enhance the intraband absorption, the sample facets are polished at 45°, so that the sample can form a multipass waveguide geometry.<sup>12</sup> This technique is standard for the study of intersubband transitions in quantum wells. The photoinduced absorption measurements were performed using a double modulation technique: the interband optical pump is mechanically chopped at 3 kHz while the mirror of the spectrometer is driven at very low frequency. The modulated interferogram is filtered with a lock-in amplifier. This double modulation technique allows to measure absorptions as low as  $10^{-5}$ . The spectral resolution of the infrared measurements is  $16 \text{ cm}^{-1}$ .

## III. IDENTIFICATION OF INTRABAND TRANSITIONS

Figure 1 shows a comparison between the infrared absorption spectrum of a *n*-doped sample (27Q78) and the low-temperature photoinduced absorption spectrum of an undoped sample (A<sub>2</sub>). The two spectra correspond to the absorption in *p* polarization (half of the electric field along the *z* growth axis). Similar spectra have already been published in separate publications.<sup>12,17</sup> They are shown here for clarity and to underline the differences with the *p*-doped samples. In both cases, the absorption is asymmetric with a large broadening ( $>100 \text{ meV}$ ). The maximum of the absorption occurs around the same energy (150 meV). For the *n*-doped sample, the absorption is unambiguously attributed to electronic intraband transitions from the populated ground

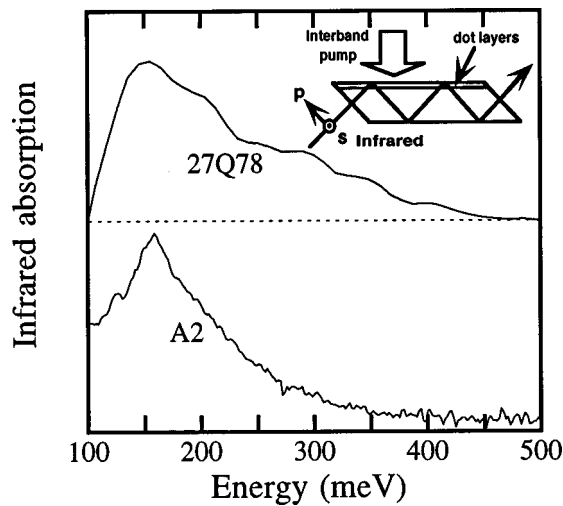


FIG. 1. Room-temperature infrared absorption of  $n$ -doped InAs/GaAs self-assembled quantum dots (27Q78) and low-temperature (15 K) photoinduced absorption of an undoped quantum dot sample ( $A_2$ ). The absorption of the  $n$ -doped sample is measured as  $1 - T_p/T_s$ , where  $T_p$  and  $T_s$  are the transmissions normalized to a GaAs substrate of the infrared in  $p$  and  $s$  polarizations, respectively. The photoinduced absorption is measured as the normalized variation of transmission with or without the interband optical excitation  $\Delta T/T$ . The photoinduced absorption vanishes beyond 400 meV which, in turn, gives the base line of the curve. The inset shows the experimental waveguide geometry and the  $p$  and  $s$  polarizations.

level. In the conduction band, only one electron state is deeply confined in the quantum dots.<sup>16,18</sup> Therefore the intraband absorption is attributed to bound-to-continuum state transitions or to transitions from the ground state to a weakly confined excited state which merges with the continuum. As the energy of the ground level strongly depends on the dot size while the onset of the continuum is weakly dependent on the dot size, the intraband absorption exhibits an inhomogeneous large broadening. Based on the similar shape and the similar energy maximum of the spectra reported in Fig. 1, it is clear that, at low temperature, the photoinduced absorption is also related to electronic bound-to-continuum intraband transition. One can define the absorption cross section for one dot layer plane following  $\alpha_z = \sigma n$ , where  $\alpha_z$  is the absorption along the  $z$  axis,  $\sigma$  the absorption cross section, and  $n$  the bidimensional carrier density which populates the dots. Assuming that all the dots are populated, the absorption cross section along the  $z$  axis is around  $3 \times 10^{-15} \text{ cm}^2$  for the intraband electronic transitions.<sup>17</sup>

One can expect, on the other hand, that the hole intraband transitions have a different signature in the mid-infrared as compared to the electron intraband transitions. Several states are confined in the valence band, due to, in particular, an heavier effective mass.<sup>16,18</sup> These states mostly have an heavy hole character although some light hole states are confined near the band edge. Note that valence band mixing between the different bulk states cannot be neglected in the 3D islands.<sup>16</sup> The striking feature is that the energy spacing between the confined hole states is weakly dependent on the dot size.<sup>16,18</sup> Therefore, one expects that the valence band intraband transitions will be dominated by bound-to-bound transitions with a small inhomogeneous broadening as compared to the electronic bound-to-continuum intraband

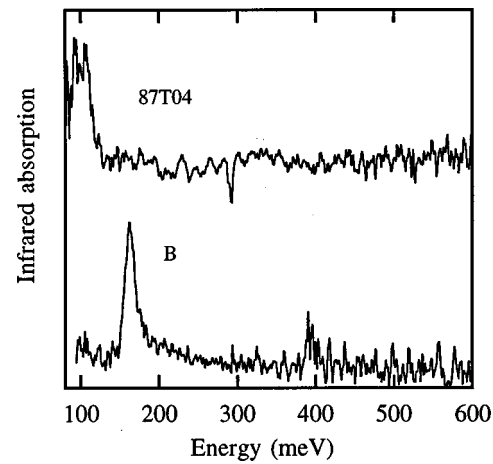


FIG. 2. Room-temperature infrared absorption of  $p$ -doped InAs/GaAs self-assembled quantum dots (87T04) and low-temperature (90 K) photoinduced absorption of an undoped quantum dot sample (sample B). The absorption of the  $p$ -doped sample is measured as  $1 - T_p/T_s$ , where  $T_p$  and  $T_s$  are the transmissions of the infrared in  $p$  and  $s$  polarizations, respectively. The photoinduced absorption vanishes beyond 450 meV which, in turn, gives the base line of the curve.

transitions. To check this point, we have investigated the intraband absorption in a  $p$ -doped sample (sample 87T04). This absorption is reported in Fig. 2 along with the photoinduced absorption of an undoped sample (sample B). As expected, the  $p$ -doped sample exhibits intraband absorption between confined states with a lower broadening ( $\sim 30 \text{ meV}$ ) than in the conduction band ( $\sim 130 \text{ meV}$ ). This feature is a signature of the bound-to-bound hole intraband absorption for the investigated InAs clusters. The absorption is polarized along the  $z$  growth axis as for the conduction intraband transitions. We can observe that the photoinduced absorption of sample B has also a reduced broadening ( $\sim 15 \text{ meV}$ ). This similitude in broadening shows that the photoinduced absorption of sample B is likely to be related to a hole intraband transition. The assignment of sample B absorption to a hole transition was previously deduced from the temperature dependence of the absorption.<sup>12</sup> The observation of photoinduced hole intraband absorption instead of electronic intraband absorption in sample B is a consequence of the sample temperature. Photoinduced electronic intraband absorption is observed more easily at low temperature, which is the case for sample  $A_2$  in Fig. 1. On the other hand, photoinduced hole intraband absorption dominates at intermediate temperature, which is the case for sample B.<sup>12</sup> For the  $p$ -doped sample, the absorption cross section  $\sigma_z$  is around  $3 \times 10^{-15} \text{ cm}^2$  which is equivalent to the absorption cross section measured in the conduction band. We can observe that the integrated intraband absorption is larger for the  $n$ -doped sample than for the  $p$ -doped sample.

#### IV. EXCITATION SPECTROSCOPY OF THE INTRABAND ABSORPTION

The dependence of the photoinduced intraband absorption on the pump photon energy is reported in Fig. 3. The experiment has been performed at 100 K on sample B and the investigated intraband absorption corresponds to a reso-

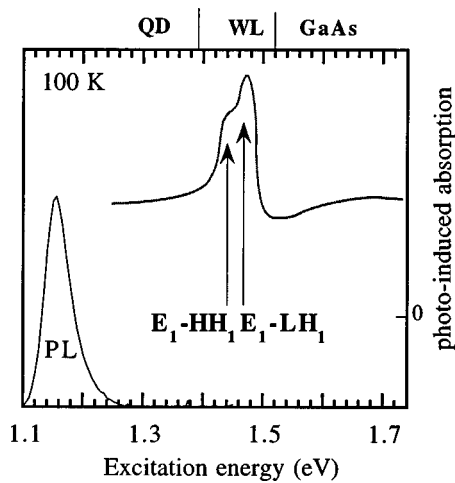


FIG. 3. Amplitude of the photoinduced intraband absorption around 160 meV of sample B vs the interband pump photon energy. The absorption is maximum when the carriers are generated in the wetting layer. The experiment is performed at 100 K. The low-temperature photoluminescence of sample B is given as a reference.

nant hole intraband transition, as reported in Sec. III. The interband optical pump is delivered by a tunable Ti:sapphire laser. As seen, the amplitude of the photoinduced intraband absorption exhibits a maximum when the interband pump photon energy is tuned in resonance with the wetting layer absorption energy. The two maxima correspond to the photon absorption in the 2D layer between  $E_1$ - $HH_1$  and  $E_1$ - $LH_1$ . For a fixed pump power, the photoinduced population of the dots is maximum when the carriers are created in the 2D wetting layer and subsequently captured in the dots. In the case of photoluminescence excitation spectroscopy,<sup>8</sup> a similar enhancement is observed with a photoluminescence maximum when the carriers are generated by absorption from the heavy hole and light hole ground subbands to the ground electronic subband. We note here that the photoinduced intraband absorption is nonvanishing when the carriers are directly generated in the quantum dots, either via absorption with the excited states or absorption with the ground states of the islands.<sup>12</sup>

## V. RESONANT EXCITATION OF THE DOTS: PHOTOLUMINESCENCE

We have first investigated the resonant excitation of the nanometer-scale quantum dots by PL. For these experiments, the quantum dots are optically excited with an energy close to the ground state energy of the clusters and the photoluminescence is recorded at energies below the excitation line. The resonant photoluminescence results from a convolution between the interband absorption, the carrier relaxation inside the dots and the interband radiative recombination. The low-temperature resonant PL spectra are reported in Fig. 4 for different excitation energies. The photoluminescence exhibits some well-defined peaks with maxima at 35, 70, 100, and 150 meV below the excitation energy and a weaker resonance around 120 meV. It appears that, at low temperature, the resonant excitation of the dots leads to a selective population of the quantum dots. For example, only the large dots

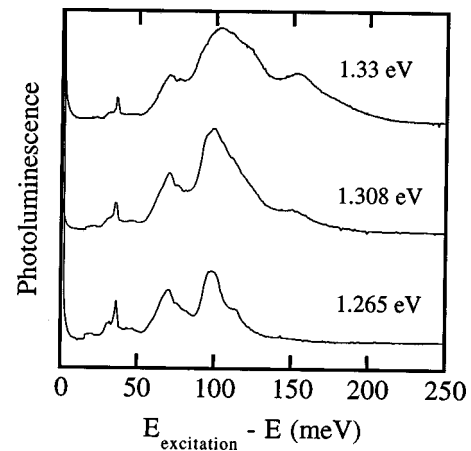


FIG. 4. 17 K resonant photoluminescence of sample A<sub>2</sub> selectively excited at different energies. From top to bottom: 1.33, 1.308, and 1.265 eV excitation energy.

are efficiently populated when the pump is set at 1.265 eV. Two types of maxima can be distinguished: the first type corresponds to the maxima around 35 and 70 meV with energy positions which do not change when the pump photon energy is varied over the 1.26–1.33 eV energy range. The second type corresponds to the maxima around 100, 120, and 150 meV which follow a slight increase  $\sim 5$  meV when the photon energy is varied from 1.26 to 1.33 eV. The amplitude of the different maxima depends on the pump wavelength and is directly related to the population efficiency of the dots. In the present experimental conditions, the photoluminescence amplitude is always maximum at 100 meV below the excitation energy. Similar spectra have already been reported in the literature.<sup>8,9,15</sup> The first peak located at 35 meV below the pump energy is very sharp and most likely attributed to a Raman resonance.<sup>6</sup> In Ref. 8–9, the other replica have been attributed to a signature of the multiphonon relaxation processes in the quantum dots since the energy of the photoluminescence peaks correspond to the sum of different phonon energies and since the energy of the PL peaks do not change when the pump excitation is varied. Note that the multiphonon relaxations involve both electron and hole relaxations, with an energy difference (electron+hole) which matches an integral number of LO-phonon energies. Regarding the origin of these spectral features and the connection with carrier relaxation processes, we underline that the assignment of the multiphonon relaxation is not straightforward. In the InAs/GaAs system, many optical phonons including bulk and interface modes in InAs and GaAs can be involved with distinct energies.<sup>18</sup> A resonance around 100 meV can be obtained by different sets of optical phonon energies. Besides, acoustic phonons can play a role in the relaxation as evidenced by recent time-resolved photoluminescence measurements.<sup>5</sup> Furthermore, recent magneto-optical studies<sup>19</sup> have shown that the phonon-related features observed in photoluminescence excitation at high energy ( $3 \times 28$ –84 meV) were in fact electronic in origin, as underlined in Ref. 16. In our experiments, we observe that the peak maxima around 100, 120, and 150 meV shift towards higher energy when the excitation energy increases (i.e.

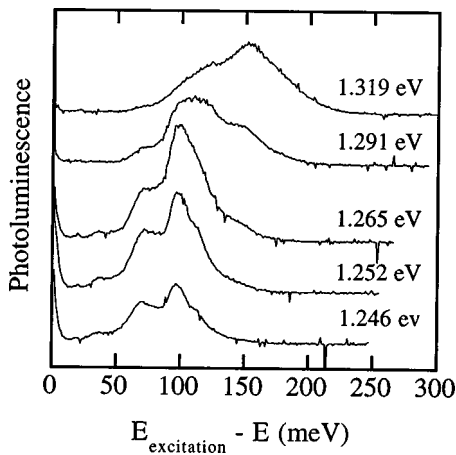


FIG. 5. 120 K resonant photoluminescence of sample  $A_2$  for different excitation energies. From top to bottom: 1.319, 1.291, 1.265, 1.252, and 1.246 eV excitation energy.

when smaller dots are excited). Therefore, these peaks are not likely to be related to multiphonon processes. In Sec. VI, we will see that the study of intraband absorption leads to an interpretation of their origin.

When the temperature is increased, resonant excitation leads to similar photoluminescence spectra. This feature is illustrated in Fig. 5 which shows the 120 K resonant photoluminescence at various interband excitation energies. The energy positions of the maxima with respect to the excitation line are similar to those observed at low temperature although the resonances are less marked. Again the relative amplitudes of the peaks depend on the excitation wavelength. We can observe that for an excitation at 1.246 eV, the broadening of the photoluminescence is only slightly reduced as compared to the nonresonantly excited photoluminescence. It indicates that the excited dot distribution is not markedly different from the dot distribution excited with an high energy laser beam. This absence of drastic change is partly due to the limit of tunability of the  $\text{Ar}^+$ -pumped Ti:sapphire laser which prevents optical pumping in the center of the dot size distribution.

## VI. RESONANT EXCITATION OF THE DOTS: INTRABAND ABSORPTION

We have performed experiments similar to the resonant photoluminescence excitation but looking at the intraband absorption. Most measurements were done on sample  $A_2$  at 120 K. At this temperature, the hole resonant intraband transitions are clearly evidenced by photoinduced absorption. At lower temperature, the infrared absorption is dominated by the electronic transition.<sup>12</sup> The infrared absorption spectra recorded for different excitation energies are reported in Fig. 6. The carriers are generated either in the substrate, in the wetting layer, or in the quantum dots via absorption in the excited levels. As reported previously, the absorption is dominated by the  $p$ -polarized absorption.<sup>12</sup> The spectra exhibit two resonant peaks at 120 and 150 meV. As opposed to the resonant photoluminescence measurements, the energy position of the peaks and their relative amplitudes are almost independent of the pump wavelength and the spectra remain

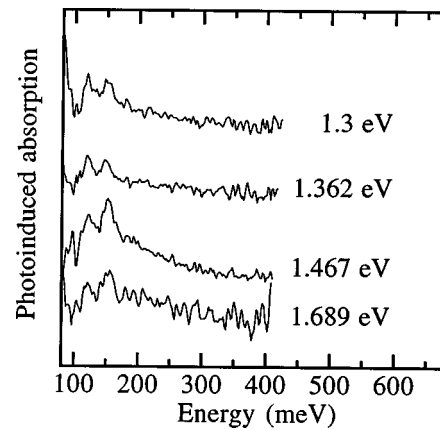


FIG. 6. 120 K photoinduced absorption  $\Delta T/T$  of sample  $A_2$  in  $p$  polarization. The absorption is measured for different interband excitation energies which correspond to photon absorption between the excited states of the dots (1.3, 1.362 eV), in the 2D wetting layer (1.467 eV) and in the substrate (1.689 eV).

identical when the sample is pumped at 1.291, 1.265, and 1.252 eV. The spectral broadening of the intraband absorption lines is  $\sim 15$  meV. The resonant absorption peaks are attributed to hole intraband transitions which occur from the ground state of the InAs clusters.<sup>12</sup> These resonant transitions are tentatively assigned to the transitions between the ground state  $|000\rangle$  to the  $|110\rangle$  (120 meV) and  $|001\rangle$  (150 meV) excited states. The notation  $(i,j,k)$  corresponds to the number of nodes presented by the envelope wave functions along the  $x$ - $y$ - $z$  spatial directions. The two resonant absorption peaks are superimposed on a broad absorption band which corresponds to the bound-to-continuum electron transitions of the dots.

The striking feature of the resonant intraband absorption is its weak dependence upon the pump wavelength. This feature is characteristic of intraband transitions as opposed to interband transitions. In the latter case, the energy spacing between the electron and hole ground states is strongly dependent on the confinement associated with the dot size. This variation is at the origin of the large broadening observed in the photoluminescence spectra. On the contrary, the energy spacing between the hole confined states is weakly dependent on the dot size. This feature has already been reported in different types of numerical simulations.<sup>16,18</sup> It explains why the position of the intraband maxima do not significantly change with the resonant excitation wavelength although the distribution of the excited dots is modified. The experimental energy shift of the intraband transition is of the order of 3 meV towards lower energy for either an optical pumping at 1.653 eV or a resonant excitation of the dots. As observed in Sec. V, the broadening of the PL is only slightly reduced when the excitation is in resonance with the quantum dots. The slight narrowing of the PL is explained by the fact that the small dots are not excited when the pump energy decreases. Only a fraction of the small dots is thus not populated in the case of the resonant pumping. The observed redshift is consistent with the decrease of the intraband energy when the average dot size increases. However, due to the resolution and the limited sensitivity of the experiment, one

cannot distinguish some secondary maxima on the intraband resonances like those observed in PL measurements.

It is important to observe that the direct comparison between the energy position of the maxima in resonantly excited PL and intraband absorption measurements is not evident. First, the interband and intraband optical transitions have distinct selection rules. Secondly, the assignment of the transitions in the interband absorption or resonant photoluminescence spectra is not straightforward: (i) in the literature, the interband spectra have been attributed either to transitions from the electron ground state to hole states<sup>8</sup> or to transitions between several electron states to hole states.<sup>4</sup> These different observations can be explained by the different size and shape of the dots which modify the predicted number of confined electron and hole states which are involved in the interband absorption. (ii) The energy dependence of the scattering rate can influence the energy position and the amplitude of the peaks observed in resonantly excited photoluminescence. (iii) Phonon-assisted absorption has also to be considered.

In the case of sample  $A_2$  studied here, the resonant PL exhibits at 120 K several maxima, as discussed in Sec. V. The resonances are broad, but for the 1.319 eV pump excitation energy, the maxima are unambiguously around 152 and 120 meV. At low temperature and for a 1.33 eV pump excitation energy, we also observe a maximum around 152 meV and a weak resonance around 120 meV. The question arises if a correlation exists between the resonant PL energy maxima and the infrared absorption maxima. The 152 and 120 meV resonances correspond to the absorption of the photons between the excited levels of the dots followed by the nonradiative relaxation inside the dots and the interband radiative recombination of the carriers between the ground states. The excited levels which are involved in the interband absorption process stem either from the conduction states, or from the valence states, or from both the conduction and valence states. It is noticeable that, in the same conditions of excitation, the intraband resonances between the valence states are observed at energies close to 120 and 150 meV, energies which correspond to the PL maxima discussed in Sec. V. Therefore, we can postulate that the interband resonances evidenced in resonant photoluminescence measurements stem from the ground electron state to the excited hole states of the clusters. It indicates that the interband absorption has a nonvanishing matrix element between the electron ground state and the  $|110\rangle$  and  $|001\rangle$  excited hole states. Interband transitions between the electronic ground state and excited hole states have already been evidenced for pyramidal-shape quantum dots.<sup>3</sup> In the present case, we experimentally show that such transitions are also allowed in the case of lens-shaped quantum dots. These experiments show the utility of both interband and intraband measurements to disentangle the electronic energy structure of the quantum dots and to identify the nature of the excited states.

In the case of the PL resonance lying at  $\sim 100$  meV below the excitation line, we have already noticed that its energy position also shifts with the interband pump energy. However, we did not observe any resonant intraband absorption around 100 meV. We postulate that this resonance stems

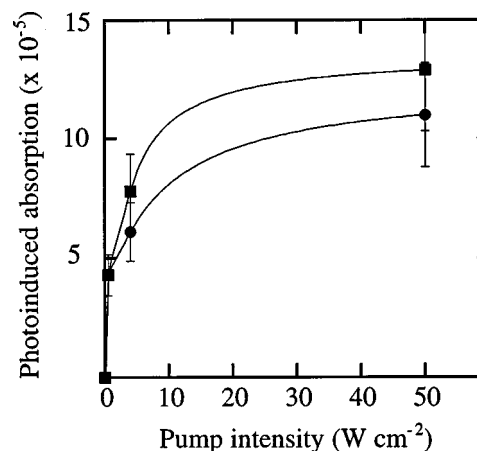


FIG. 7. 120 K amplitude ( $\Delta T/T$ ) of the intraband peaks at 120 (dots) and 150 meV (squares) for sample  $A_2$  vs the interband pump intensity. The interband pump energy is 1.362 eV and corresponds to an excitation between the excited states of the dots. The full curves are guides to the eye.

from an interband transition involving an excited electron state and an excited hole state, most probably a transition between the doubly degenerate  $|100\rangle$  hole state to the doubly degenerate  $|100\rangle$  electron state.

## VII. PUMP INTENSITY INFLUENCE ON INTRABAND ABSORPTION

The magnitude of the two resonant intraband transitions observed in sample  $A_2$  vs the interband pump intensity is reported in Fig. 7. The cw measurements were done at 120 K with the interband pump excitation energy set at 1.362 eV. The interband photons are thus absorbed between the excited levels of the clusters. Both transitions follow the same dependence as a function of the pump intensity. The ratio between the absorption amplitudes is almost constant for the investigated interband pump intensities. It confirms that the two transitions originate from the same ground level of the dots. The amplitude of the intraband absorption follows a sublinear law and saturates above  $20 \text{ W cm}^{-2}$ . We have checked that in similar conditions, the photoluminescence starts to broaden for intensities which are also in the  $20 \text{ W cm}^{-2}$  intensity range. This broadening is a signature of the state filling of the dots which corresponds to a saturation of the ground level population. At this point, the excited levels start to be populated and participate to the photoluminescence. The ground state filling of the dots can thus be either evidenced by photoluminescence or by photoinduced infrared absorption. A similar saturation behavior has been observed for an interband excitation in resonance with the wetting layer band gap. It indicates that the saturation is not the consequence of the excitation of a particular class of quantum dots.

The number of carriers which are present in the dots can be estimated from the magnitude of the intraband absorption. Assuming that the cross section along the  $z$  axis of the intraband absorption is around  $1.5 \times 10^{-15} \text{ cm}^2$  for a one dot layer plane,<sup>12,20</sup> the number of injected carriers  $n$  can be deduced from

$$\frac{\Delta T}{T} = N_p \sigma_z n \frac{S_{\text{pump}}}{S_{\text{infrared}}}, \quad (1)$$

where  $N_p$  is the number of quantum dot layer planes,  $n$  the bidimensional carrier density, and  $S_{\text{pump}}$  and  $S_{\text{infrared}}$  the surfaces of the interband pump and infrared probe beams, respectively. For a  $50 \text{ W cm}^{-2}$  pump intensity at 1.362 eV and a ratio  $S_{\text{pump}}/S_{\text{infrared}} \sim 0.5$ , it yields a bidimensional carrier density  $n \sim 5 \times 10^9 \text{ cm}^{-2}$ .

The injected carrier density can also be deduced from rate equations. In the linear absorption regime, the carrier density is given by  $n = G\tau$ , where  $G = \alpha I/h\nu$  is the generation rate,  $\alpha$  the absorption probability,  $I$  the pump intensity,  $h\nu$  the photon energy, and  $\tau$  the interband recombination lifetime. Assuming  $\alpha = 10^{-2}$ ,  $I = 50 \text{ W cm}^{-2}$  at 1.362 eV, and  $\tau \sim 1.5 \text{ ns}$ , we find an injected carrier density  $n \sim 3.4 \times 10^9 \text{ cm}^{-2}$ , a density of the same order of magnitude than the previously estimated ground state carrier density in the dots. However, we would expect a much higher value for the total injected carrier density in the dots since we observe in Fig. 7 a saturation below  $50 \text{ W cm}^{-2}$ . A possible explanation is that the  $\tau \sim 1.5 \text{ ns}$  effective lifetime is underestimated at 120 K since it does not account for the thermal escape of the carriers out of the dots.<sup>21</sup> Note that the photoinduced infrared absorption is expected to be proportional to the electron density in the ground state of the dots. Thus one expects the photoinduced absorption to follow a linear behavior vs pump intensity up to the filling of the ground states and to be constant at higher intensities. A surprising feature is that we did not observe a linear dependence even at low pump intensity. This feature could indicate again that the thermal escape of the carriers from the islands plays a significant role at 120 K.

The question arises why photoluminescence and photoinduced intraband absorption exhibit a saturation behavior at carrier densities which are one order of magnitude lower than the nominal dot density. A possible explanation is that, at 120 K, the dot density involved in photoluminescence and in photoinduced intraband absorption is lower than the nominal dot density. As a matter of fact, the PL and intraband saturation intensities are about one order of magnitude larger in the case of sample B.<sup>12</sup> Therefore the assumption of a lower dot density for sample A<sub>2</sub> as compared to a standard sample is not unrealistic. Moreover, as underlined in Sec. II, sample A<sub>2</sub> stems from a region close to the 2D-3D growth mode transition. It is thus not surprising to find experimentally a lower dot density.<sup>13,14</sup>

### VIII. CONCLUSION

In summary, we have investigated interband and intraband transitions in self-assembled quantum dots. The inter-

band transitions have been studied by resonantly excited photoluminescence. The intraband transitions have been evidenced by photoinduced infrared spectroscopy using a resonant excitation. The spectral features of the electron and hole intraband transitions (energy position, broadening) have been evidenced. Our work shows the advantage of studying both the interband and intraband transitions in quantum dots to unambiguously assign the nature of the excited states involved in the absorption processes.

### ACKNOWLEDGMENT

This work was supported by DGA under Contract No. 97062/DSP.

- <sup>1</sup>J.-Y. Marzin, J.-M. Gérard, A. Izraël, D. Barrier, and G. Bastard, *Phys. Rev. Lett.* **73**, 716 (1994).
- <sup>2</sup>M. Grundmann *et al.*, *Phys. Rev. Lett.* **74**, 4043 (1995).
- <sup>3</sup>M. Grundmann, N. N. Ledentsov, O. Stier, D. Bimberg, V. M. Ustinov, P. S. Kop'ev, and Zh. I. Alferov, *Appl. Phys. Lett.* **68**, 979 (1996).
- <sup>4</sup>K. H. Schmidt, G. Medeiros-Ribeiro, M. Oestreich, P. M. Petroff, and G. H. Döhler, *Phys. Rev. B* **54**, 11346 (1996).
- <sup>5</sup>B. Ohnesorge, M. Albrecht, J. Oshinowo, A. Forchel, and Y. Arakawa, *Phys. Rev. B* **54**, 11532 (1996).
- <sup>6</sup>J. M. Gérard, J. Y. Marzin, G. Zimmermann, A. Ponchet, O. Cabrol, D. Barrier, B. Jusserand, and B. Sermage, *Solid-State Electron.* **40**, 807 (1996).
- <sup>7</sup>N. Nirmal, C. B. Murray, and M. G. Bawendi, *Phys. Rev. B* **50**, 2293 (1994).
- <sup>8</sup>R. Heitz *et al.*, *Appl. Phys. Lett.* **68**, 361 (1996).
- <sup>9</sup>M. J. Steer, D. J. Mowbray, W. R. Tribe, M. S. Skolnick, M. D. Sturge, M. Hopkinson, A. G. Cullis, C. R. Whitehouse, and R. Murray, *Phys. Rev. B* **54**, 17738 (1996).
- <sup>10</sup>Ch. Sikorski and U. Merkt, *Phys. Rev. Lett.* **62**, 2164 (1989).
- <sup>11</sup>H. Drexler, D. Leonard, W. Hansen, J. P. Kotthaus, and P. M. Petroff, *Phys. Rev. Lett.* **73**, 2252 (1994).
- <sup>12</sup>S. Sauvage, P. Boucaud, F. H. Julien, J.-M. Gérard, and J.-Y. Marzin, *J. Appl. Phys.* **82**, 3396 (1997).
- <sup>13</sup>D. Leonard, K. Pond, and P. M. Petroff, *Phys. Rev. B* **50**, 11687 (1994).
- <sup>14</sup>J.-M. Gérard, J. B. Génin, J. Lefebvre, J. M. Moison, N. Lebouché, and F. Barthe, *J. Cryst. Growth* **150**, 351 (1995).
- <sup>15</sup>S. Fafard, R. Leon, D. Leonard, J. L. Merz, and P. M. Petroff, *Phys. Rev. B* **52**, 5752 (1995).
- <sup>16</sup>M. A. Cusack, P. R. Briddon, and M. Jaros, *Phys. Rev. B* **56**, 4047 (1997).
- <sup>17</sup>S. Sauvage, P. Boucaud, F. H. Julien, J. M. Gérard, and V. Thierry-Mieg, *Appl. Phys. Lett.* **71**, 2785 (1997).
- <sup>18</sup>M. Grundmann, O. Stier, and D. Bimberg, *Phys. Rev. B* **52**, 11969 (1995).
- <sup>19</sup>L. R. Wilson, D. J. Mowbray, M. S. Skolnick, M. Morifuji, M. J. Steer, I. A. Larkin, and M. Hopkinson, *Phys. Rev. B* **57**, R2073 (1998).
- <sup>20</sup>This absorption cross section is lower than the absorption cross section of sample 87T04. This discrepancy is partly attributed to a difference of dot shapes between the two samples.
- <sup>21</sup>M. Gurioli, A. Vinattieri, M. Colocci, C. Deparis, J. Massies, G. Neu, A. Bosacchi, and S. Franchi, *Phys. Rev. B* **44**, 3115 (1991).